

RAPID REPORT

Transmembrane AMPA receptor regulatory protein regulation of competitive antagonism: a problem of interpretation

David M. MacLean and Derek Bowie

Department of Pharmacology and Therapeutics, McGill University, Montréal, Québec, Canada

Non-technical summary Communication between neurons is often carried out by neurotransmitters, such as glutamate, and their receptor proteins, such as AMPA-type glutamate receptors. It has become clear that these AMPA receptors are not alone in cell membranes but are often associated with auxiliary proteins which alter their responsiveness to blocking drugs. In particular, the transmembrane AMPA receptor regulatory protein (TARP) family of auxiliary proteins has been argued to make the receptor less sensitive to antagonists and more sensitive to neurotransmitter. Here we apply basic pharmacological principles to argue that these two effects are not separate but linked to each other, i.e. AMPA receptors are less sensitive to antagonists *because* they are more sensitive to neurotransmitter. We further highlight that when considering the very rapid nature of signalling between nerve cells, neurotransmitters have insufficient time to dislodge antagonists from their binding site. As a result, antagonists *appear* to work through a different mechanism.

Abstract Synaptic AMPA receptors are greatly influenced by a family of transmembrane AMPA receptor regulatory proteins (TARPs) which control trafficking, channel gating and pharmacology. The prototypical TARP, stargazin (or $\gamma 2$), shifts the blocking ability of several AMPAR-selective compounds including the commonly used quinoxalinedione antagonists, CNQX and NBQX. Stargazin's effect on CNQX is particularly intriguing as it not only apparently lowers the potency of block, as with NBQX, but also renders it a partial agonist. Given this, agonist behaviour by CNQX has been speculated to account for its weaker blocking effect on AMPAR–TARP complexes. Here we show that this is not the case. The apparent effect of stargazin on CNQX antagonism can be almost entirely explained by an increase in the apparent affinity for L-glutamate (L-Glu), a full agonist and neurotransmitter at AMPAR synapses. Partial agonism at best plays a minor role but not through channel gating *per se* but rather because CNQX elicits AMPAR desensitization. Our study reveals that CNQX is best thought of as a non-competitive antagonist at glutamatergic synapses due to the predominance of non-equilibrium conditions. Consequently, CNQX primarily reports the proportion of AMPARs available for activation but may also impose additional block by receptor desensitization.

(Submitted 25 August 2011; accepted after revision 29 September 2011; first published online 3 October 2011)

Corresponding author D. Bowie: Department of Pharmacology & Therapeutics, Bellini Building, Room 164, McGill University, 3649 Promenade Sir William Osler, Montreal, Québec, Canada H3G 0B1. Email: derek.bowie@mcgill.ca

Abbreviations CTZ, cyclothiazide; eGFP, enhanced green fluorescent protein; iGluR, ionotropic glutamate receptor; KA, kainate; LBD, ligand-binding domain; TARP, transmembrane AMPA receptor regulatory protein.

Introduction

Selective pharmacological tools have been crucial in advancing the understanding of specific roles of ionotropic glutamate receptors (iGluRs). Among the most useful are compounds from the quinoxalinedione family, of which CNQX is perhaps the best known and most widely used. Since the late-1980s, CNQX has been employed as a useful competitive antagonist of AMPA- and kainate (KA)-type iGluRs (Honore *et al.* 1988). However, recent studies using stargazin (or $\gamma 2$), the prototypical TARP, show that TARPs are so effective in promoting channel opening (Tomita *et al.* 2005) that they convert the minimal free energy of CNQX binding into activation (Menuz *et al.* 2007). These findings explain earlier studies showing that CNQX may not be a pure competitive antagonist in a neuronal setting (McBain *et al.* 1992; Brickley *et al.* 2001; Maccaferri & Dingledine, 2002) and has also prompted others to investigate the ability of stargazin and other TARPs to convert CNQX into a weak partial agonist (Cokic & Stein, 2008; Kott *et al.* 2009).

However, these studies have examined how TARPs modify CNQX action under equilibrium conditions where CNQX and L-Glu achieve steady-state occupancy. At glutamatergic synapses, however, L-Glu duration in the cleft is too brief to reach steady state (Wyllie & Chen, 2007). Therefore, the relevant issue is how TARPs might alter CNQX block in non-equilibrium conditions. In addition to focusing on equilibrium conditions, previous work has only ever examined the ability of CNQX to gate AMPARs. However, a hallmark of most AMPAR agonists is rapid and near-complete desensitization. It is not yet known if CNQX accesses high-affinity desensitized states upon binding to AMPARs.

In this study we re-examine the effect of stargazin on the inhibitory potency of both CNQX and NBQX. We find that their reduced ability to block AMPARs bound by stargazin is not due to a change in quinoxalinedione binding as proposed by others (Kott *et al.* 2007; Cokic & Stein, 2008). Instead, kinetic simulations suggest that it is an indirect effect which can be almost entirely explained by an increase in apparent agonist affinity. We further show that under non-equilibrium conditions, which dominate at glutamatergic synapses, CNQX and NBQX effectively behave as non-competitive antagonists and continue to block AMPAR-TARP complexes with high affinity. CNQX differs from NBQX, however, in that some of the block observed with CNQX is due to receptor desensitization.

Methods

Cell culture and transfection

All experiments described in this study were performed on outside-out patches excised from transfected tsA201

cells as described previously (MacLean *et al.* 2011). Briefly, cDNAs encoding enhanced green fluorescent protein (eGFP), the GluA1 AMPAR subunit and/or stargazin were transiently transfected using the calcium phosphate method at ratios of (eGFP:GluA1:stargazin) 1:10:15 or 1:10:20 for 10–14 h. We included 10 μM NBQX in the media to inhibit cell death. eGFP-expressing cells were used for electrophysiology 24–48 h later.

Electrophysiology

Outside-out patch recordings were performed using borosilicate glass pipettes of 3–5 M Ω coated with dental wax, fire-polished and filled with a solution which contained (mM): 115 NaCl, 10 NaF, 10 Na₂ATP, 5 Na₄BAPTA, 5 Hepes, 1 MgCl₂ and 0.5 CaCl₂, which was adjusted to pH 7.4 with 5 N NaOH and 295 mosmol l⁻¹ with sucrose. External solutions were composed of (mM): 150 NaCl, 5 Hepes, 0.1 MgCl₂ and 0.1 CaCl₂, and adjusted to pH 7.4 with 5 N NaOH and 295 mosmol l⁻¹ with sucrose. CNQX activation curves described in Fig. 3 were performed in solutions of high ionic strength to better resolve the small membrane currents. These internal solutions contained (mM): 365 NaCl, 10 NaF, 10 Na₂ATP, 5 Na₄BAPTA, 5 Hepes, 1 MgCl₂ and 0.5 CaCl₂ (pH 7.4), and the external solution was composed of 400 NaCl, 5 Hepes, 0.1 MgCl₂ and 0.1 CaCl₂ (pH to 7.4). Osmolarity was adjusted to 755 mosmol l⁻¹ in both solutions.

AMPARs were activated by 10 mM L-glutamate every 5 s and CNQX every 10 s. All recordings were performed using an Axopatch 200B amplifier (Molecular Devices, Sunnyvale, CA, USA) acquired at 50–100 kHz and filtered at 10 kHz (8-pole Bessel) under the control of pCLAMP9 software (Molecular Devices). Series resistances (3–12 M Ω) were routinely compensated by >95%, and solution exchange time was determined at the end of each experiment by measuring the liquid junction current (10–90% rise time of 50–200 μs). Drugs were purchased from Tocris (MI, USA) and stored as frozen stocks in external solution at –20°C. All experiments were performed at room temperature.

Data analysis

Inhibition curves to CNQX or NBQX shown in Fig. 2 were fitted assuming a single binding site isotherm of the form:

$$I = (I_{\text{max}} / (1 + ([\text{antagonist}] / \text{IC}_{50})^n)) \quad (1)$$

where I_{max} is the peak current occurring at time t_{peak} in the absence of antagonist, I is the response at t_{peak} for a given antagonist concentration ($[\text{antagonist}]$), IC_{50} is the concentration required for 50% inhibition and n is the slope.

CNQX dose–response curves shown in Fig. 3 were fitted with the logistic equation of the form:

$$I = I_{\max}/(1 + (EC_{50}/[\text{agonist}])^n) \quad (2)$$

where I_{\max} is the extrapolated maximal response from fits of the data points, I is the equilibrium response to a given agonist concentration ($[\text{agonist}]$), EC_{50} is the concentration which produces 50% of the maximal response and n is the slope. All fitting was performed using Clampfit 9.0 or Origin 7.0. When mentioned, statistical significance was assessed using a Student's t test.

Simulations of an AMPA receptor gating model

Kinetic simulations of an AMPAR gating model were performed to examine how stargazin affects agonist and antagonist sensitivity (Fig. 4). To do this, we identified a series of rate constants that simulated the functional properties of the GluA1 AMPAR alone or when bound by stargazin. Rate constants were obtained using two software tools. We used Channel Lab 2.0 (Synaptosoft) with Runge–Kutta numerical integration to approximate desensitization kinetics and FACILE v0.25 (courtesy of Julien Ollivier) (Siso-Nadal *et al.* 2007) in combination with purpose-written Matlab code (7.8, MathWorks) to perform multiple simulations of desensitization, peak and steady-state glutamate dose–response curves and CNQX inhibition curves as shown in Fig. 4.

Importantly, the models used are not intended to reproduce every aspect of AMPAR–TARP gating. For example, we did not consider the effect of CNQX on channel activation, desensitization or co-activation by glutamate and CNQX. Nor did we determine to what extent the TARP-induced increase in agonist potency is due to an increase in agonist affinity (smaller k_{-1}), efficacy (larger β) or the promotion of larger sub-conductance states (Tomita *et al.* 2005). The precise details of how TARPs alter AMPAR gating are beyond the scope of this study (e.g. Milstein *et al.* 2007). The essential point is that an increase in steady-state agonist potency by any mechanism results in a decrease in antagonist potency at equilibrium.

Results

CNQX block of AMPARs can appear to be non-competitive

CNQX was first reported to be a potent competitive antagonist of non-NMDA receptors after it was shown to selectively inhibit responses elicited by kainate (KA) and quisqualate but not NMDA (Honore *et al.* 1988). Subsequent work revealed that CNQX had a high affinity for AMPARs primarily due to its slow rate of unbinding

(Clements *et al.* 1998; Rosenmund *et al.* 1998). The slow dissociation rate means that CNQX remains bound to AMPARs (residency time >100 ms; Clements *et al.* 1998) far longer than the duration of a single AMPAR activation (~ 10 ms; Zhang *et al.* 2008). As a result, CNQX antagonism of AMPAR-mediated synaptic events will not reach equilibrium as is often assumed (Wyllie & Chen, 2007). Instead, the slow unbinding of CNQX and fast kinetics of AMPARs means that block will *appear* to be non-competitive, even though CNQX is a competitive antagonist.

To illustrate this point, we measured the inhibition of peak L-glutamate (L-Glu) responses to a concentration of CNQX reported to produce half-maximal block (Colquhoun *et al.* 1992). Figure 1A and B illustrate the results of this experiment showing that 100 nM CNQX inhibited responses elicited by 10 mM L-Glu at GluA1 AMPARs by approximately 50% (Fig. 1A). As expected of an apparent non-competitive antagonism, the degree of block was unchanged even when the agonist concentration was increased 5-fold to 50 mM (Fig. 1B). This finding is consistent with the fact that CNQX dissociates far too slowly from AMPARs for competitive block to occur during the brief time course of receptor activation.

Competition can be observed, however, if CNQX and L-Glu are permitted to reach steady-state occupancy. To illustrate this, we performed recordings in the continual presence of CNQX and compared inhibition within the first millisecond (black circles, Fig. 1C and D) and after 1 s of AMPAR activation where equilibrium conditions with CNQX are established (grey circles, Fig. 1C and D). Visual inspection of the L-Glu-evoked responses shown in Fig. 1C supports this reasoning. Using cyclothiazide (CTZ, 100 μM) to enhance the resolution of the AMPAR equilibrium response, membrane current relaxations show two distinct kinetic components: a rapidly rising response over the first 0.5 ms which reflects AMPAR activation, and a second much slower phase which corresponds to the re-equilibration of CNQX block (Fig. 1C). Measurement of CNQX antagonism shortly after receptor activation (black circles) and once equilibrium conditions had been met (grey circles) (Fig. 1C), reveals that the degree of block is time-dependent. In support of this, the IC_{50} value for responses measured shortly after receptor activation was 280 ± 20 nM ($n_H = 0.81 \pm 0.05$) whereas inhibition was shifted about 250-fold to 70 ± 4 μM ($n_H = 0.63 \pm 0.02$) under equilibrium conditions, demonstrating that the potency of block is substantially weakened as L-Glu and CNQX reach steady-state occupancy (Fig. 1D). As noted by others (Wyllie & Chen, 2007), this principle is significant because recent studies examining the effect of TARPs on CNQX block of AMPARs have all performed their experiments under equilibrium conditions (Kott *et al.* 2007; Cokic & Stein, 2008). However, the relevant

issue at central synapses is how CNQX behaves in non-equilibrium conditions. Given this, we re-examined the effect of TARPs on CNQX block.

TARPs do not substantially alter antagonist potency of quinoxalinediones

Competitive block of AMPARs by CNQX is shifted as much as 10-fold in the presence of the TARP stargazin (Kott *et al.* 2007; Cokic & Stein, 2008). To determine if a similar shift occurs under non-equilibrium conditions, we compared the inhibitory effect of CNQX on rapid L-Glu activations of GluA1 AMPARs alone and when co-assembled with stargazin (Fig. 2). We confirmed the presence of AMPAR–stargazin complexes in our

recordings by their enhanced steady-state response to L-Glu (Fig. 2A right panel, arrow). Contrary to previous studies, co-expression of GluA1 AMPARs with stargazin only shifted the potency of CNQX block by about 2-fold (IC_{50} , 220 ± 30 nM, $n = 5-17$) compared to AMPARs alone (IC_{50} , 110 ± 10 nM, $n = 4-12$) (Fig. 2A and B). This weak effect is not unique to CNQX since we also failed to observe an appreciable shift in block potency by another quinoxalinedione, NBQX. In this case, the potency of NBQX block was also modestly affected by stargazin with IC_{50} values at GluA1 AMPARs of 6.6 ± 0.4 nM ($n = 3-6$) and the IC_{50} at AMPAR–stargazin complexes of 12.6 ± 1.2 nM ($n = 4-10$) (Fig. 2B). Interestingly, stargazin significantly reduced the slope (n_H) of the inhibition curve for CNQX from 1.1 ± 0.1 for GluA1 alone to 0.8 ± 0.1 in

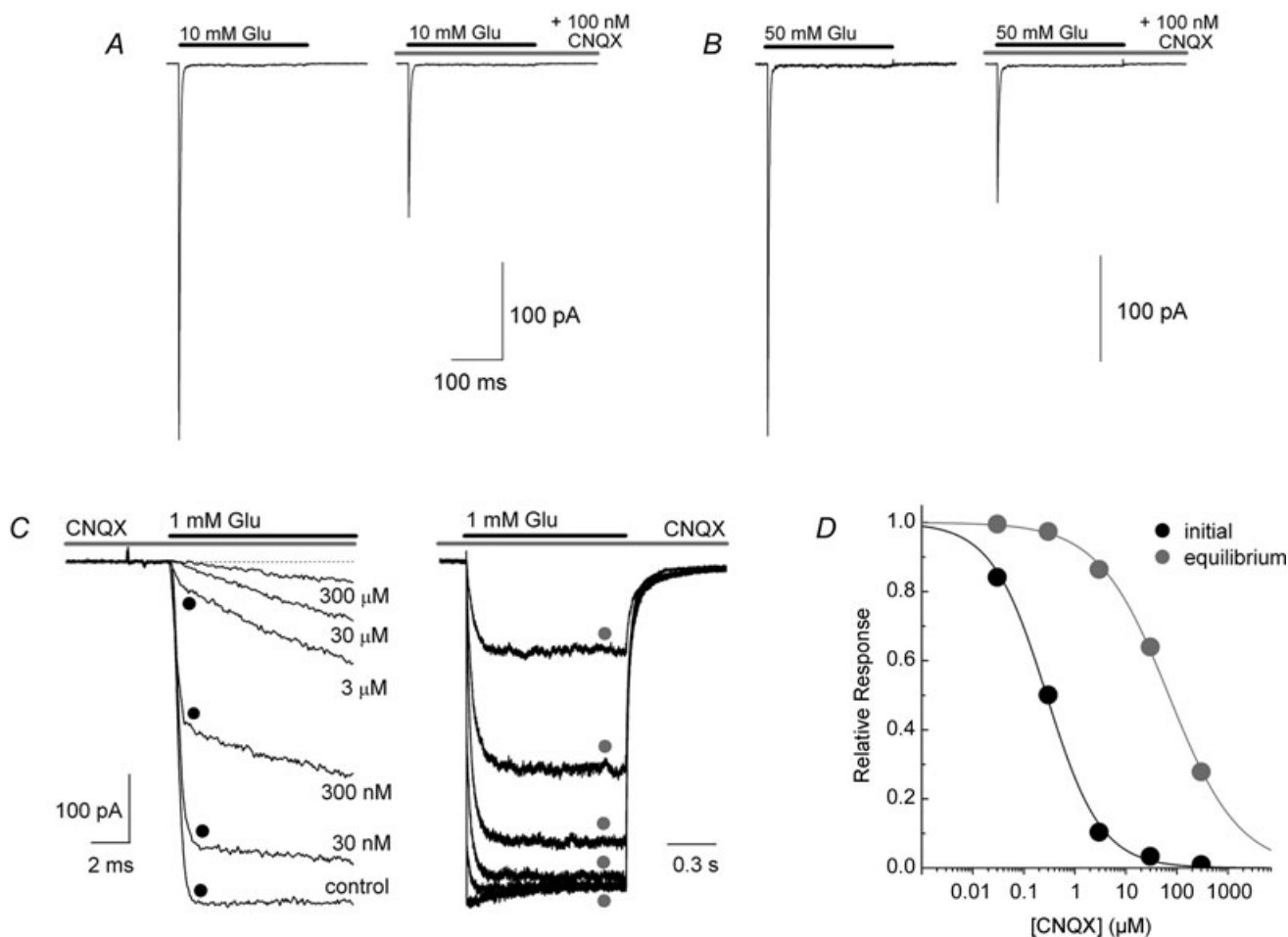


Figure 1. CNQX block can be competitive and appear non-competitive

A and B, membrane currents elicited by applications of 10 (A) and 50 mM L-Glu (B) on a patch containing GluA1 (patch no. 091006p5). Note that the degree of block observed with 100 nM CNQX was identical in each case. C, left, initial fast component of a series of L-Glu responses on an outside-out patch in the continual presence of cyclothiazide ($100 \mu\text{M}$). Each trace represents the response in different background concentrations of CNQX (30 nM– $300 \mu\text{M}$) (patch no. 110129p4). C, right, same recording but now showing the entire 1 s agonist application and the slower re-equilibration kinetics of CNQX block. D, inhibition plots of the experiment in C shows that CNQX block of the initial response has a higher affinity than at equilibrium.

the presence of stargazin (Fig. 2*B*) which was not observed with NBQX (n_H , 1.0 ± 0.1 for GluA1 alone; 1.1 ± 0.1 with stargazin, Fig. 2*B*). As discussed below, this finding prompted us to examine if the blocking mechanism may reflect the ability of CNQX to also gate the AMPAR.

Partial agonism by CNQX does not contribute to high-affinity block of AMPARs

Partial agonist behaviour by CNQX has been proposed to account for the shift in equilibrium block at AMPAR-stargazin complexes (Cokic & Stein, 2008). To estimate the influence of partial agonism in our experiments, we examined the degree of overlap between the ability of CNQX to inhibit AMPARs (Fig. 2) with its ability to activate them (Fig. 3), which was determined by constructing dose-response curves (Fig. 3). To better resolve CNQX-evoked membrane currents which were small in amplitude in outside-out patches, we modified the recording conditions in two ways. First, we conducted

our experiments in 400 mM NaCl to increase the driving force through the channel. Second, we noticed that CNQX, but not NBQX, caused appreciable macroscopic desensitization (% desensitization, $88 \pm 3\%$; time course, $\tau = 7.3 \pm 1.5$ ms, Fig. 3*A* right panel) that has not been reported previously. Because of this, we performed our experiments in the continual presence of CTZ which increased peak CNQX responses by approximately 2-fold to $7.1 \pm 1.6\%$ of the L-Glu peak (Fig. 3*A* and *B*).

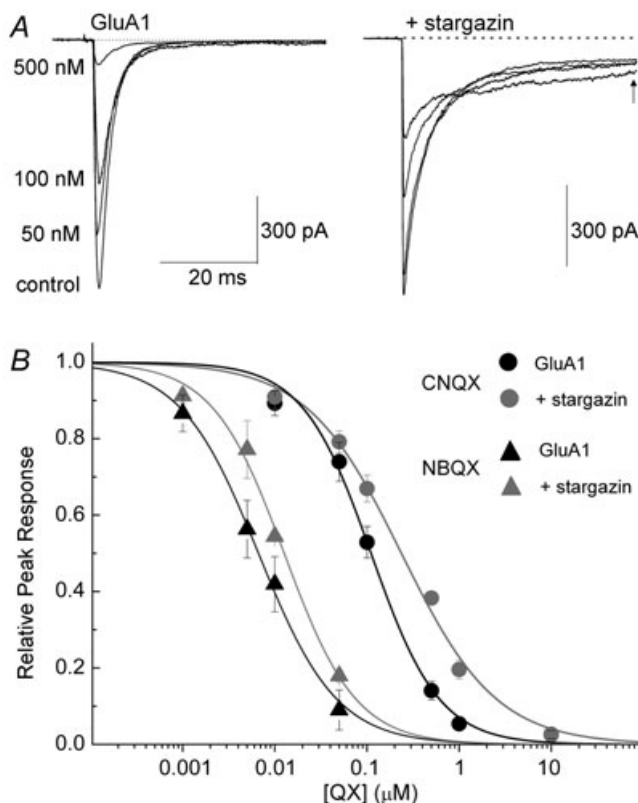


Figure 2. Stargazin does not substantially alter the blocking ability of CNQX or NBQX

A, inhibitory effect of CNQX on responses evoked by 10 mM L-Glu on patches of GluA1 alone (patch no. 070827p1) or with GluA1 and stargazin (patch no. 070817p1). *B*, inhibition plots of block by CNQX (circles, $n = 4-17$) and NBQX (triangles, $n = 3-10$) of peak L-Glu responses evoked from patches containing GluA1 alone (black) or with stargazin (grey).

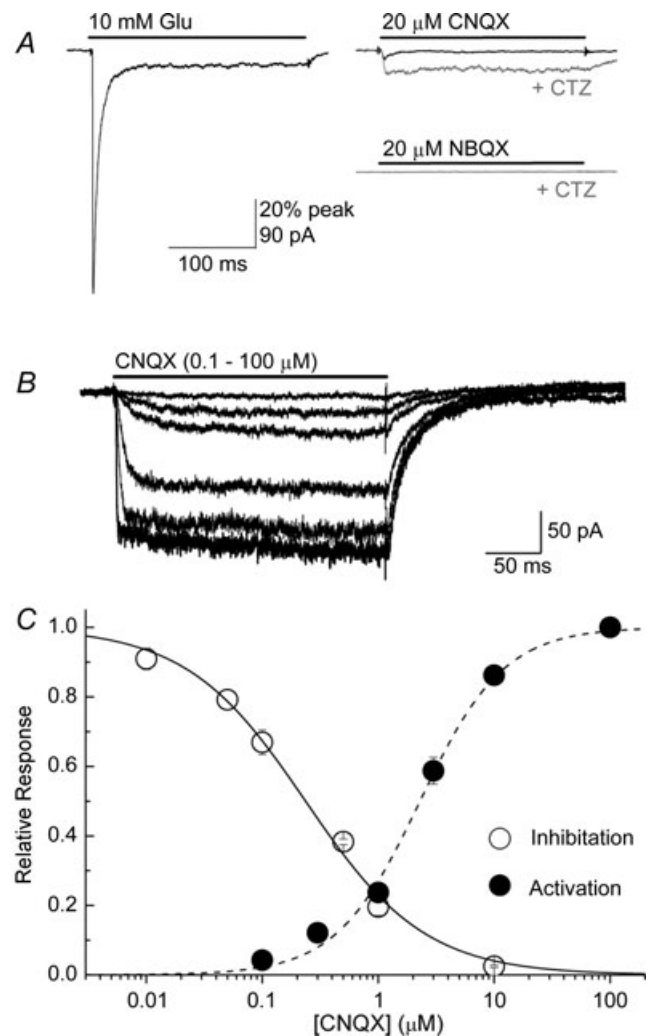


Figure 3. Activation or desensitization by CNQX contributes little to high-affinity AMPAR block

A, left, response from a patch containing GluA1 and stargazin to 10 mM L-Glu (patch no. 080201p1). *A*, right, responses from the same patch to 20 μ M CNQX (upper) or 20 μ M NBQX (lower) either alone (black) or in the continual presence of 100 μ M CTZ (grey). *B*, responses from GluA1 with stargazin to varying concentrations of CNQX in the presence of CTZ and with 400 mM NaCl (patch no. 110216p1). *C*, summary of inhibition curve for GluA1 plus stargazin from Fig. 2 and activation curve for CNQX in the continual presence of CTZ.

Under these conditions, CNQX activated GluA1/stargazin channels with an EC_{50} of $2.3 \pm 0.2 \mu\text{M}$ and slope (n_H) of 1.2 ± 0.1 ($n = 4-5$, Fig. 3) which was an order of magnitude higher than its potency as a blocker (IC_{50} , $220 \pm 30 \text{ nM}$) (Fig. 2). Since CTZ causes a leftward shift in the apparent affinity for AMPAR agonists (Partin *et al.* 1996), the overlap between CNQX's blocking ability and action as a partial agonist is most probably overestimated in these experiments. Given this, we conclude that block observed under non-equilibrium conditions is not greatly influenced by the action of CNQX as a partial agonist. Since CNQX also elicits AMPAR desensitization, this property may play a role in the blocking mechanism. However, as described below, the reported effects of stargazin on CNQX block can be almost entirely explained by a leftward shift in the apparent agonist affinity.

Stargazin reduces CNQX block by increasing agonist potency

How might stargazin shift CNQX block by as much as 10-fold under equilibrium conditions but exhibit only a modest effect when block is non-competitive? Estimates of IC_{50} values determined under equilibrium conditions are agonist-concentration dependent (Wyllie & Chen, 2007). Consequently, it is possible that stargazin affects the potency of CNQX not by a direct effect on the antagonist but by causing a shift in (apparent) agonist affinity. In support of this, several studies have already established that TARPs increase the potency of L-Glu at AMPARs (Tomita *et al.* 2005; Cokic & Stein, 2008; Kott *et al.* 2009).

To examine the relationship between agonist potency and CNQX block, we performed kinetic simulations of a two-binding site, single open state gating model

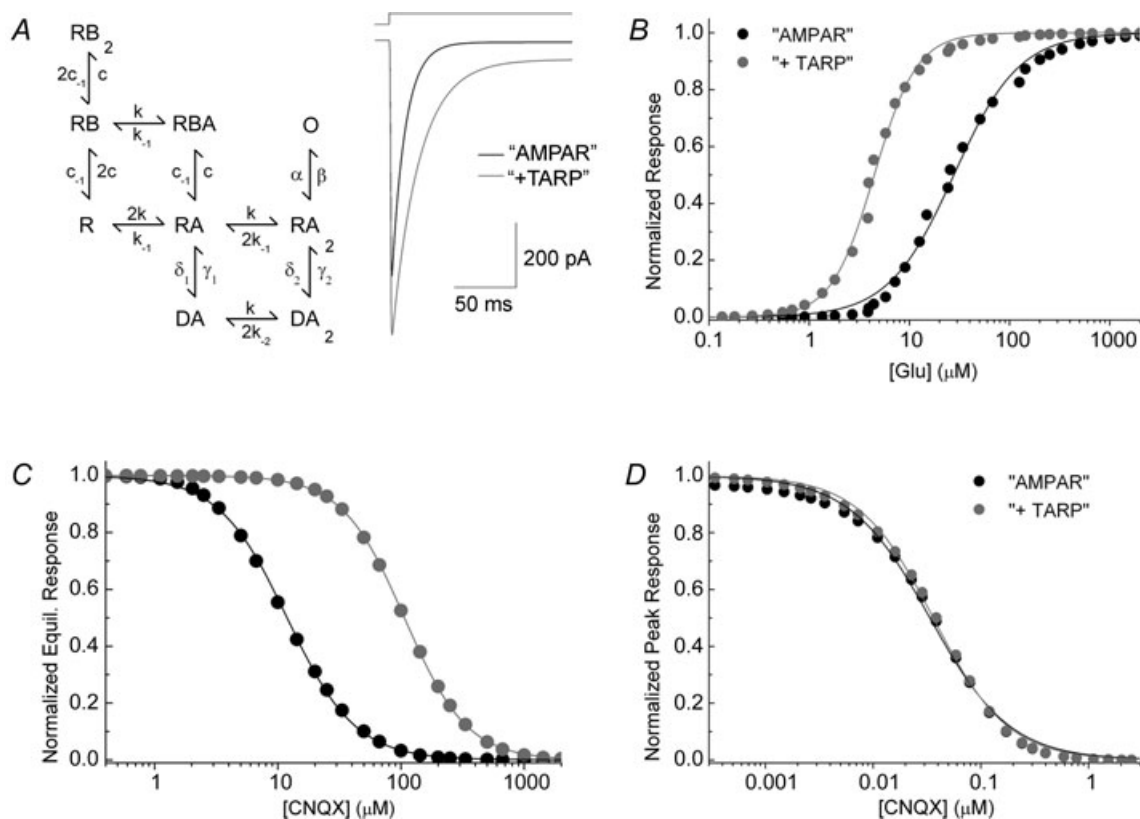


Figure 4. Stargazin reduces CNQX block by increasing agonist potency

A, left, gating scheme used in all simulations. In the reaction scheme, each binding site, denoted R, can be bound by either an agonist (A) or a blocker (B). D denotes a desensitized state and O is the open state. For the 'AMPA' model, the rate constants were (in s^{-1}): $k = 3.6 \times 10^7 \text{ M}^{-1}$; $k_{-1} = 15,000$; $k_{-2} = 360$; $c = 3.6 \times 10^7 \text{ M}^{-1}$; $c_{-1} = 2.3$; $\beta = 20,000$; $\alpha = 1600$; $\gamma_1 = 3.5$; $\delta_1 = 200$; $\gamma_2 = 3.5$ and $\delta_2 = 8300$. The rate constants for the '+TARP' model were identical except: $k_{-1} = 1000$; $k_{-2} = 48$; $\beta = 50,000$; $\gamma_1 = 11$; $\delta_1 = 131$; $\gamma_2 = 14.7$ and $\delta_2 = 7350$. B, simulations of dose-response relationships for equilibrium responses for 'AMPA' and '+TARP' models. C, simulated inhibition curves for equilibrium responses using $250 \mu\text{M}$ L-Glu. D, simulated inhibition curves for peak 10 mM L-Glu responses in the same models. Note that the curves are almost identical.

that mimics key functional properties of the GluA1 AMPAR alone or AMPAR–TARP complexes as reported by others (Fig. 4A) (Robert & Howe, 2003; Tomita *et al.* 2005; Cokic & Stein, 2008; Kott *et al.* 2009). For the GluA1 AMPAR model, the rate constants used gave appropriate desensitization decays ($\tau = 2.2$ ms), steady-state amplitude (0.8% of peak) and steady-state dose–response curve (EC_{50} of $30 \mu\text{M}$ and $n_H = 1.33$) (Fig. 4A, right and 4B), consistent with published work (Robert & Howe, 2003; Tomita *et al.* 2005; Cokic & Stein, 2008; Kott *et al.* 2009). Rate constants for the AMPAR–TARP model were determined by first increasing the open rate of the channel (Morimoto-Tomita *et al.* 2009) and destabilizing the desensitized states as previously suggested (Milstein *et al.* 2007) which resulted in appropriate slowing of decay kinetics ($\tau = 4.7$ ms) and enhanced steady-state response (about 7% of peak response) (Fig. 4A, right). L-Glu unbinding rates were then reduced to simulate the increase in apparent agonist affinity produced by stargazin (EC_{50} of $4.4 \mu\text{M}$, $n_H = 2$) (Fig. 4B) (Tomita *et al.* 2005; Cokic & Stein, 2008; Kott *et al.* 2009; Morimoto-Tomita *et al.* 2009). Finally, competitive inhibition by CNQX was then added to the ‘AMPA’ model by choosing rate constants for CNQX dissociation to obtain an IC_{50} of $10 \mu\text{M}$ ($n_H = 1.5$) observed under equilibrium conditions with $250 \mu\text{M}$ L-Glu, thus reflecting results and experimental conditions of previous studies (Cokic & Stein, 2008; Kott *et al.* 2009).

To examine the degree of CNQX block in the ‘+TARP’ model, we used the same set of rate constants for CNQX as in the ‘AMPA’ model. As hypothesized, this produced a reduction in inhibitory potency of CNQX giving an IC_{50} of $110 \mu\text{M}$ ($n_H = 1.71$) representing an 11-fold shift (Fig. 4C). This simulation suggests that the reduction in antagonist potency may be entirely independent of CNQX’s binding properties but rather a consequence of increased agonist potency observed with AMPAR–stargazin complexes. Importantly, if the peak response (and not equilibrium activation) is simulated using saturating agonist concentrations (i.e. 10 mM L-glutamate), virtually no shift in inhibitory potency is observed (Fig. 4D) with both models yielding IC_{50} values of approximately 35 nM ($n_H = 1.2$). Consequently, we conclude that the apparent shift in potency at equilibrium seen by others can be attributed solely to an increase in L-Glu potency, although we cannot exclude some minor direct alteration to CNQX affinity (see Discussion).

Discussion

Here we report three important findings that advance our understanding of how CNQX works at glutamatergic synapses. First, CNQX appears to behave in a non-competitive manner in conditions found at glutamatergic synapses due to its slow dissociation

rate from AMPARs (Fig. 1). As a result, CNQX inhibition of peak responses reports the fraction of AMPARs that are available for activation. Second, we show that CNQX is able to induce macroscopic desensitization of AMPAR–stargazin complexes (Fig. 3) which may play a minor role in the blocking mechanism. Third, stargazin does not substantially alter the potency of quinoxalinedione block of AMPARs under non-equilibrium or equilibrium conditions (Fig. 2). The apparent shift in CNQX potency seen by others in equilibrium conditions can be wholly attributed to increased agonist potency by stargazin (Fig. 4).

Does stargazin alter the apo state of the AMPAR to slow quinoxalinedione binding?

In our experiments, stargazin lowered NBQX and CNQX block of AMPARs by about 2-fold (Fig. 2B) which was not predicted by the gating model (Fig. 4D). How might this occur? There are two possibilities: stargazin accelerates CNQX unbinding or slows binding. It seems unlikely that TARPs accelerate CNQX unbinding as they slow deactivation rates (Priel *et al.* 2005; Milstein *et al.* 2007), and increase agonist potency, both of which are suggestive of slower, not faster, unbinding rates. Furthermore, faster CNQX dissociation requires that TARPs reduce the stability of the CNQX-bound closed conformation of the ligand-binding domain (LBD). Arguing against this idea is that greater stability of the LBD closed-cleft conformations enhances agonist efficacy at AMPARs (Zhang *et al.* 2008) and perhaps kainate receptors (MacLean *et al.* 2011) and TARPs increase agonist efficacy (Tomita *et al.* 2005). Consequently, it is unlikely that TARPs accelerate unbinding of CNQX or NBQX.

The alternative possibility is that TARPs slow binding rates by modifying the apo conformation(s) of the AMPAR LBDs. Indeed, a very attractive hypothesis is that TARPs modify AMPAR gating by promoting a slightly more closed apo conformation of the LBD (Landes *et al.* 2011). Such TARP-promoted apo states would require less free energy from ligand binding to enter stable closed-cleft states, resulting in easier channel opening and increased efficacy. Moreover, apo states which begin closer to ‘active’ and away from ‘desensitized’ conformations may explain the slower desensitization rate and extent seen with TARPs (Tomita *et al.* 2005; Milstein *et al.* 2007). In this model, the binding rates for smaller ligands like L-Glu and KA might be unaffected by subtle increases in apo cleft closure but larger compounds like the quinoxalinedione would bind slower, resulting in the small but consistent shifts in inhibition curves (Fig. 2). It will be interesting in future studies to test if TARPs do indeed stabilize slightly more closed apo conformations of AMPAR LBDs.

References

- Brickley SG, Farrant M, Swanson GT & Cull-Candy SG (2001). CNQX increases GABA-mediated synaptic transmission in the cerebellum by an AMPA/kainate receptor-independent mechanism. *Neuropharmacology* **41**, 730–736.
- Clements JD, Feltz A, Sahara Y & Westbrook GL (1998). Activation kinetics of AMPA receptor channels reveal the number of functional agonist binding sites. *J Neurosci* **18**, 119–127.
- Cokic B & Stein V (2008). Stargazin modulates AMPA receptor antagonism. *Neuropharmacology* **54**, 1062–1070.
- Colquhoun D, Jonas P & Sakmann B (1992). Action of brief pulses of glutamate on AMPA/kainate receptors in patches from different neurones of rat hippocampal slices. *J Physiol* **458**, 261–287.
- Honore T, Davies SN, Drejer J, Fletcher EJ, Jacobsen P, Lodge D & Nielsen FE (1988). Quinoxalinediones: potent competitive non-NMDA glutamate receptor antagonists. *Science* **241**, 701–703.
- Kott S, Sager C, Tapken D, Werner M & Hollmann M (2009). Comparative analysis of the pharmacology of GluR1 in complex with transmembrane AMPA receptor regulatory proteins $\gamma 2$, $\gamma 3$, $\gamma 4$, and $\gamma 8$. *Neuroscience* **158**, 78–88.
- Kott S, Werner M, Korber C & Hollmann M (2007). Electrophysiological properties of AMPA receptors are differentially modulated depending on the associated member of the TARP family. *J Neurosci* **27**, 3780–3789.
- Landes CF, Rambhadran A, Taylor JN, Salatan F & Jayaraman V (2011). Structural landscape of isolated agonist-binding domains from single AMPA receptors. *Nat Chem Biol* **7**, 168–173.
- McBain CJ, Eaton JV, Brown T & Dingledine R (1992). CNQX increases spontaneous inhibitory input to CA3 pyramidal neurones in neonatal rat hippocampal slices. *Brain Res* **592**, 255–260.
- Maccaferri G & Dingledine R (2002). Complex effects of CNQX on CA1 interneurons of the developing rat hippocampus. *Neuropharmacology* **43**, 523–529.
- MacLean DM, Wong AY, Fay AM & Bowie D (2011). Cations but not anions regulate the responsiveness of kainate receptors. *J Neurosci* **31**, 2136–2144.
- Menuz K, Stroud RM, Nicoll RA & Hays FA (2007). TARP auxiliary subunits switch AMPA receptor antagonists into partial agonists. *Science* **318**, 815–817.
- Milstein AD, Zhou W, Karimzadegan S, Brecht DS & Nicoll RA (2007). TARP subtypes differentially and dose-dependently control synaptic AMPA receptor gating. *Neuron* **55**, 905–918.
- Morimoto-Tomita M, Zhang W, Straub C, Cho CH, Kim KS, Howe JR & Tomita S (2009). Autoinactivation of neuronal AMPA receptors via glutamate-regulated TARP interaction. *Neuron* **61**, 101–112.
- Partin KM, Fleck MW & Mayer ML (1996). AMPA receptor flip/flop mutants affecting deactivation, desensitization, and modulation by cyclothiazide, aniracetam, and thiocyanate. *J Neurosci* **16**, 6634–6647.
- Priel A, Kollerker A, Ayalon G, Gillor M, Osten P & Stern-Bach Y (2005). Stargazin reduces desensitization and slows deactivation of the AMPA-type glutamate receptors. *J Neurosci* **25**, 2682–2686.
- Robert A & Howe JR (2003). How AMPA receptor desensitization depends on receptor occupancy. *J Neurosci* **23**, 847–858.
- Rosenmund C, Stern-Bach Y & Stevens CF (1998). The tetrameric structure of a glutamate receptor channel. *Science* **280**, 1596–1599.
- Siso-Nadal F, Ollivier JF & Swain PS (2007). Facile: a command-line network compiler for systems biology. *BMC Syst Biol* **1**, 36.
- Tomita S, Adesnik H, Sekiguchi M, Zhang W, Wada K, Howe JR, Nicoll RA & Brecht DS (2005). Stargazin modulates AMPA receptor gating and trafficking by distinct domains. *Nature* **435**, 1052–1058.
- Wyllie DJ & Chen PE (2007). Taking the time to study competitive antagonism. *Br J Pharmacol* **150**, 541–551.
- Zhang W, Cho Y, Lolis E & Howe JR (2008). Structural and single-channel results indicate that the rates of ligand binding domain closing and opening directly impact AMPA receptor gating. *J Neurosci* **28**, 932–943.

Author contributions

D.B. and D.M.M. designed the research and D.M.M. performed the experiments which were carried out at McGill University, Montreal. Both authors contributed to writing the manuscript and approved the final version.

Acknowledgements

This work was supported by operating grants from the CIHR to D.B. D.M.M. is supported by a Canada Graduate Scholarship and Standard Life Scholarship. D.B. is the recipient of a Canada Research Chair award. We wish to thank Drs Julien Ollivier and Peter Swain for use of the FACILE software.